





Estimation of Intraglomerular Pressure Using Invasive Renal Arterial Pressure and Flow Velocity Measurements in Humans

Didier Collard ¹, Peter M. van Brussel,² Lennart van de Velde ^{1,3}, Gilbert W.M. Wijnjens,² Berend E. Westerhof ⁴, John M. Karemaker,⁵ Jan J. Piek,² Jim A. Reekers,⁶ Liffert Vogt ⁷, Robbert J. de Winter,² and Bert-Jan H. van den Born¹

Due to the number of contributing authors, the affiliations are listed at the end of this article.

ABSTRACT

Background Glomerular hyperfiltration resulting from an elevated intraglomerular pressure (Pglom) is an important cause of CKD, but there is no feasible method to directly assess Pglom in humans. We developed a model to estimate Pglom in patients from combined renal arterial pressure and flow measurements.

Methods We performed hemodynamic measurements in 34 patients undergoing renal or cardiac angiography under baseline conditions and during hyperemia induced by intrarenal dopamine infusion (30 μ g/kg). For each participant during baseline and hyperemia, we fitted an adapted three-element Windkessel model that consisted of characteristic impedance, compliance, afferent resistance, and Pglom.

Results We successfully analyzed data from 28 (82%) patients. Median age was 58 years (IQR, 52–65), median eGFR was 95 ml/min per 1.73 m² (IQR, 74–100) using the CKD-EPI formula, 30% had microalbuminuria, and 32% had diabetes. The model showed a mean Pglom of 48.0 mm Hg (SD=10.1) at baseline. Under hyperemia, flow increased by 88% (95% CI, 68% to 111%). This resulted in a 165% (95% CI, 79% to 294%) increase in afferent compliance and a 13.1-mm Hg (95% CI, 10.0 to 16.3) decrease in Pglom. In multiple linear regression analysis, diabetes (coefficient, 10.1; 95% CI, 5.1 to 15.1), BMI (0.99 per kg/m²; 95% CI, 0.38 to 1.59), and renal perfusion pressure (0.42 per mm Hg; 95% CI, 0.25 to 0.59) were significantly positively associated with baseline Pglom.

Conclusions We constructed a model on the basis of proximal renal arterial pressure and flow velocity measurements that provides an overall estimate of glomerular pressure and afferent and efferent resistance in humans. The model provides a novel research technique to evaluate the hemodynamics of CKD on the basis of direct pressure and flow measurements.

Clinical Trial registry name and registration number Functional HEmodynamics in patients with and without Renal Artery stenosis (HERA), NL40795.018.12 at the Dutch national trial registry (toetsingonline.nl).

JASN 31: 1905–1914, 2020. doi: <https://doi.org/10.1681/ASN.2019121272>

The development of CKD and its progression to ESKD remain a major source of reduced quality of life and significant mortality.¹ Glomerular hyperfiltration resulting from an elevated intraglomerular pressure (Pglom) is an important factor in the pathogenesis of CKD and hypertension-mediated kidney damage.² The importance of hyperfiltration is widely accepted in different disease

Received December 10, 2019. Accepted April 19, 2020.

Published online ahead of print. Publication date available at www.jasn.org.

Correspondence: Dr. Bert-Jan H. van den Born, Department of Vascular Medicine, Amsterdam University Medical Centers, University of Amsterdam, Location AMC, PO Box 22660, 1100 DD Amsterdam, The Netherlands. Email: b.j.vandenborn@amsterdamumc.nl

Copyright © 2020 by the American Society of Nephrology

states, including diabetic nephropathy, essential hypertension, and FSGS secondary to early kidney injury.^{3,4} An increase in Pglom can be a direct consequence of impaired autoregulation in patients with hypertension or diabetes, or it can occur along the common pathway of progressive glomerulosclerosis toward ESKD.⁵ Prevention of glomerular hyperfiltration by adequate hypertension control and renin-angiotensin system inhibition in patients with diabetes or proteinuria is widely recommended in current guidelines to prevent progression of CKD.^{6,7} Recent studies have shown the renoprotective effect of SGLT-2 inhibitors, which are likely in part mediated through alterations of renal hemodynamics.⁸ Studies using para-aminohippurate clearance showed in patients with type 1 diabetes that GFR was reduced as a result of a reduction in renal plasma flow, whereas in patients with type 2 diabetes, GFR was reduced because of decreased filtration.^{9,10} This suggests that SGLT-2 inhibition can alter Pglom, with different effects depending on patient characteristics. However, although direct measurements can be obtained in animal models using micropuncture techniques,^{11–14} measurement of absolute Pglom in humans is not feasible. Until now, only the Gomez equations have been used for estimation of Pglom in humans on the basis of measures of GFR, which only yield estimates relative to an assumed average Pglom of 60 mm Hg.¹⁵

Direct assessment of renal hemodynamics using combined intrarenal pressure and flow velocity measurements may provide further insight in renal pathophysiology and serve as a benchmark for future noninvasive diagnostics in patients with CKD.^{16,17} Recently, we have shown that measurement of intrarenal hyperemic flow velocity during dopamine-induced hyperemia is feasible and reproducible.¹⁸ The renal circulation consists of afferent and efferent arteriolar systems, which can more or less independently influence GFR. Therefore, it is important to separate afferent from efferent vessels in order to determine their effect on glomerular filtration and kidney oxygenation.¹² In animal models of the renal circulation, renal flow is usually measured in steady state under varying perfusion pressure.¹⁹ Because it is difficult to directly change renal perfusion pressure during measurements in humans without invoking autoregulatory mechanisms, we developed a model describing instantaneous renal pressure and flow using the dynamics within one heartbeat by combining a three-element Windkessel model with a pressure offset to model glomerular pressure. Windkessel models have been widely used in the systemic and pulmonary circulation: for instance, to determine systemic and pulmonary arterial compliance, estimate cardiac output, and more recently, model boundary conditions in computational fluid dynamics models of peripheral vascular disease.^{20–22} We hypothesize that adaptation of the Windkessel model to the renal circulation enables a consistent estimation of an absolute value for Pglom.²³ This is on the basis of the assumptions that (1) Pglom is more or less equal in all nephrons and can thus be described using a single-nephron model, (2) pressure pulsatility is absent in the

Significance Statement

Increased intraglomerular pressure is an important contributor to the pathogenesis and progression of CKD in patients with hypertension and diabetes. This study used an adapted Windkessel model to estimate overall renal arterial resistance, arterial compliance, and intraglomerular pressure based on intrarenal pressure and flow velocity measurements in patients undergoing angiography. The mean intraglomerular pressure was consistent with values in non-human primates. It decreased following hyperemia with efferent exceeding afferent dilatation and had significant positive correlation with perfusion pressure and diabetes. The current model and its derived parameters provide a new research technique to assess the renal hemodynamic effects of therapeutic interventions.

glomerulus, and (3) the Windkessel model gives a valid description of pulsatile hemodynamics. The aim of this study was to determine the feasibility of using this adapted Windkessel method to assess renal and glomerular hemodynamics in a heterogeneous population of patients with and without renovascular disease by determining Pglom, renal arterial compliance, and afferent and efferent resistances.

METHODS

Study Design and Participants

We used data of 34 participants from the functional renal HEodynamics in patients with and without Renal Artery stenosis (HERA) study included between March 2014 and April 2019 with successful hemodynamic measurements. The HERA study is an observational cohort study performed at the Amsterdam University Medical Centers (location Academic Medical Center), for which the methods have been described in detail elsewhere.¹⁸ In brief, additional intrarenal pressure and flow velocity measurements were performed in patients with a clinical indication for coronary or renal angiography. For inclusion, patients had to be between 18 and 75 years old and in a clinically stable condition. Patients with an acute coronary syndrome within 4 weeks before the procedure, severe valvular heart disease, or heart failure (NYHA Class >II) or those having an increased risk for contrast nephropathy defined as an eGFR < 30 ml/min per 1.73 m² using the Chronic Kidney Disease Epidemiology Collaboration (CKD-EPI) formula were excluded.²⁴ The study design and protocol were approved by the local ethics committee. The study has been registered under number NL40795.018.12 at the national trial registry (toetsingonline.nl). The study was conducted according to the principles of the Declaration of Helsinki and in accordance with the Medical Research involving Human Subjects Act (WMO). All patients were informed about the study procedures and procedure-related risks and provided written informed consent before participation. The data and Matlab implementation of the model that support the findings of this study are available from the corresponding author on reasonable request.

Study Measurements

Study procedures were performed after the elective coronary or renal procedure by a team of five experienced interventionists. A 5–6 French guiding catheter was advanced from either radial or femoral access to a renal artery. Patients were randomized between measurement in the left or right renal artery if no stenosis was present, using blinded envelopes. Through angiographic guidance, a 0.014-inch Doppler and pressure sensor–equipped wire (Combwire; Philips-Volcano, San Diego, CA) was positioned inside the main renal artery such that a stable pressure and flow signal were obtained. If necessary, the wire was advanced into the first branch of the renal artery to obtain a stable signal. In the presence of a stenosis, the sensor was positioned at least three vessel diameters distally from the stenosis. The Combwire was used to simultaneously measure distal pressure and flow velocity, whereas the proximal pressure was measured using the fluid-filled catheter. BP and flow velocity measurements were stored digitally at a frequency of 200 Hz using the ComboMap device (Philips-Volcano), after which offline data analysis was performed using custom written software in MATLAB (R2018b; The MathWorks, Inc.). In each patient, a baseline measurement of at least 1 minute was performed. Subsequently, hyperemia was induced by intrarenal administration of 30 $\mu\text{g}/\text{kg}$ dopamine, and a measurement of at least 10 minutes was performed.²⁵ Distal pressure and flow velocity were used for the Windkessel model. eGFR was estimated from plasma creatinine in samples obtained at the beginning of the catheterization procedure using the CKD-EPI formula.²⁴ Microalbuminuria, defined as a urinary albumin-creatinine ratio ≥ 2.5 mg/mmol for men and ≥ 3.5 mg/mmol for women, was assessed in a urine sample obtained before hemodynamic measurements.

Data Analyses

The distal pressure and flow velocity signals were filtered using a Savitzky–Golay filter, which is a low-pass filtering method on the basis of fitting polynomials to adjacent data points.²⁶ To account for the processing delay of the Doppler flow velocity signal, the flow velocity signal was shifted backward by 50 milliseconds, such that the relation between pressure and flow velocity became linear during the systolic upstroke in the pressure flow loop.²⁷ Manually, a representative sample of five to ten consecutive beats of sufficient signal quality was selected for each subject during baseline and during maximal hyperemia. From this selection, an ensemble-averaged pressure and flow velocity beat was constructed using the selected sample by taking the mean of the beats scaled to a duration of 1 second for further analysis.

We adapted a three-element Windkessel model to the renal circulation by adding an extra pressure offset variable for Pglom.²¹ This model, as described below, was used to estimate the vascular properties of the renal artery, the Pglom, and the afferent and efferent resistances. Pglom was directly compared between individuals and between conditions. The ratio between hyperemia and baseline was calculated for the

parameters of interest because flow velocity rather than volumetric flow rate was measured. This allows for comparison between participants because the ratio is not dependent on the vessel diameter. We verified model consistency by estimating Pglom using the first harmonic method, which is a commonly used technique to estimate cerebral critical closing pressure.²⁸ Additionally, we repeated the model computations for the second hyperemic reproducibility measurement in the subset where recordings of sufficient quality were available. We compared the results from our model with the Gomez equations on the basis of eGFR, plasma protein, and renal blood flow from the intrarenal measurements (Supplemental Material).

For deriving the renal Windkessel model, we first assume that all nephrons are equal in hemodynamic properties. The renal circulation can then be described by a single-nephron model consisting of an afferent arteriole, the glomerulus, and an efferent arteriole (Figure 1, lower panel).²⁹ The afferent arteriole (Figure 1, upper panel) is modeled by a three-element Windkessel consisting of a proximal resistance that models the characteristic impedance of the afferent macrovasculature in series with a capacitor modeling compliance parallel to a resistor modeling the afferent microvascular resistance.²¹ Next, we assume that the Pglom is constant during one heartbeat and that venous pressure is zero. The efferent resistance of the model is defined as the combined resistance of the efferent arteriole and peritubular capillary resistance. We denote by P and F the discrete Fourier transforms of pressure and flow velocity, respectively, and with $k = 0, 1, 2, \dots$, we denote the frequency of the corresponding harmonic in Hertz. The measured impedance is given by³⁰

$$Z(k) = \frac{\tilde{P}(k)}{F(k)}$$

The impedance is modeled by

$$Z_{Wk}(k) = \frac{R_a - Z_c}{1 + i \cdot 2\pi \cdot k \cdot (R_a - Z_c) \cdot C_T} + Z_c,$$

where i is the complex unit. Fitted model parameters are P_{glom} in millimeters of mm Hg, the characteristic impedance Z_c in mm Hg per (centimeters per second), and the compliance C_T in centimeters per mm Hg, where impedance and compliance are defined using flow velocity. The Windkessel parameters are estimated by least square minimization of the modeled and measured flow beats:

$$\varepsilon(P_{glom}, Z_c, C_T) = \sum_{t=0, \dots, 0.5} \left[\phi \left(\frac{\tilde{P}(k) - \tilde{P}_{glom}(k)}{Z_{WK}(k)} \right) (t) - F(t) \right]^2,$$

where ϕ denotes the inverse Fourier transform, $P_{glom}^{\sim}(0) = P_{glom}$, and $P_{glom}^{\sim}(k) = 0$ for $k = 1, 2, \dots$. Only the first 0.5 seconds were used for minimization because the signal-noise ratio in

the flow signal was relatively low during diastole. Adequacy of fit was checked by visually comparing the shape of the modeled impedance $Z_{Wk}(k)$ with the measured impedance $Z(k)$. Samples where the measured or fitted impedance did not have the convex downward slope as depicted in Figure 2 were excluded. The afferent resistance R_a and the efferent resistance R_e could then be computed from the fitted P_{glom} :

$$R_a = \frac{P^-(0) - P_{glom}}{F^-(0)} \quad \text{and} \quad R_e = \frac{P_{glom} - 0}{F^-(0)}.$$

Statistical Analyses

Baseline characteristics were depicted using mean or median with SD or interquartile range (IQR), respectively. Baseline and hyperemic parameters were compared using *t* tests. Ratios were log transformed before analysis and given as geometric mean and SD. The primary outcome of the model was the estimated Pglom at baseline and hyperemia. We performed univariate regression analyses to identify relevant clinical correlates with baseline Pglom, including age, sex, body mass index (BMI), eGFR, presence of microalbuminuria, history of diabetes, use of angiotensin-converting enzyme inhibitors or angiotensin receptor blockers, and renal perfusion pressure. Using backward selection on the basis of the Akaike information criterion, we derived a multiple linear regression model for baseline Pglom. The same covariates were used in the regression model for hyperemic Pglom. The intraclass correlation coefficient and a Bland–Altman analysis were used to compare the estimated Pglom using the Windkessel method with the first harmonic method. All statistical analyses were conducted with R version 3.6.1 (R Foundation, Vienna, Austria). The figures were created using R, Matlab, and Graphpad version 8.3.0.

RESULTS

We used data of 34 patients (68% men) for this analysis. Median age was 58 years (IQR, 52–65), median eGFR was 95 ml/min per 1.73 m² (IQR, 74–100), and 30% had microalbuminuria. Twenty-three (68%) patients had a history of cardiovascular disease, whereas 11 (32%) patients had diabetes, and 4 (12%) had a renal artery stenosis. Twenty-six (76%) patients used BP-lowering medication, and 21 (62%) used an angiotensin-converting enzyme inhibitor or angiotensin receptor blocker. An example of a successful fit of the Windkessel model is given in Figure 2. Of the 34 recordings that were analyzed, an adequate fit could not be obtained in six patients on the basis of visual inspection because of a low signal-noise ratio in the flow velocity measurements. There were no relevant differences in patient characteristics between participants with a successful fit and those without, and these six individuals were excluded from the analysis. An overview of the baseline characteristics is given in Table 1.

Comparison of Baseline versus Hyperemia

The results of the Windkessel model during baseline and hyperemia are depicted in Table 2. During hyperemia, renal blood flow increased by 88% (95% confidence interval [95% CI], 68% to 111%). At baseline, the estimated Pglom was 48.0 (SD=10.1) mm Hg, which declined to 34.9 (SD=8.7) mm Hg during hyperemia (difference of 13.1 mm Hg; 95% CI, 10.0 to 16.3; *P*<0.001). In patients with renal artery stenosis, similar results were observed with a mean Pglom of 48.0 mm Hg (SD=7.8) during baseline and 34.7 mm Hg (SD=6.3) during hyperemia. Afferent resistance decreased by 43% (95% CI, 35% to 51%; *P*<0.001) during hyperemia, whereas efferent resistance decreased by 62% (95% CI, 55% to 67%; *P*<0.001). The comparison between the second and first hyperemic measurements showed similar values of Pglom, with a mean difference of 1.4 mm Hg (95% CI, –9.6 to 12.4). The comparison between the renal Windkessel method and the first harmonic method gave for the latter on average a 5.1-mm Hg lower (95% CI, –13.0 to 2.8 mm Hg) Pglom compared with the Windkessel method. A Bland–Altman analysis, shown in Supplemental Figure 1, shows no additional proportional bias and overall good agreement of Pglom with an intraclass correlation coefficient of 0.94 (*P*<0.001). We found no correlation between Pglom estimated using the Gomez equations and the Windkessel model (*r* = –0.24; 95% CI, –0.75 to 0.46) (Supplemental Material, Supplemental Figure 2).

Regression Analyses

The results for the univariate and multiple regression analyses for baseline Pglom are given in Supplemental Table 1. In univariate analysis, Pglom was significantly associated with perfusion pressure (*r* = 0.51; *P* = 0.006) and the presence of diabetes (*r* = 0.49, *P* = 0.008); additionally, there was a trend with BMI (*r* = 0.31; *P* = 0.10). On the basis of the stepwise backward regression, we included only diabetes, glomerular pressure, and BMI in the multiple linear regression model. Figure 3 shows the distribution of Pglom in patients with diabetes compared with patient without diabetes. In the multiple regression model, diabetic patients had a 10.1-mm Hg higher Pglom (95% CI, 5.1 to 15.1; *P* < 0.001), which decreased to a 4.2-mm Hg difference during hyperemia (95% CI, –1.9 to 10.4; *P* = 0.17). A 1-mm Hg increase in perfusion pressure was associated with a 0.42-mm Hg increase in Pglom (95% CI, 0.25 to 0.60; *P* < 0.001). This relation disappeared during hyperemia (slope, 0.16; 95% CI, –0.06 to 0.37; *P* = 0.15). BMI was significantly associated with Pglom, with regression coefficients of 0.99 per 1-kg/m² increase in BMI (95% CI, 0.38 to 1.59; *P* = 0.003) during baseline and 1.04 (95% CI, 0.30 to 1.78; *P* = 0.008) during hyperemia.

DISCUSSION

In this study, we introduced an adapted version of the three-element Windkessel model to estimate Pglom and renal

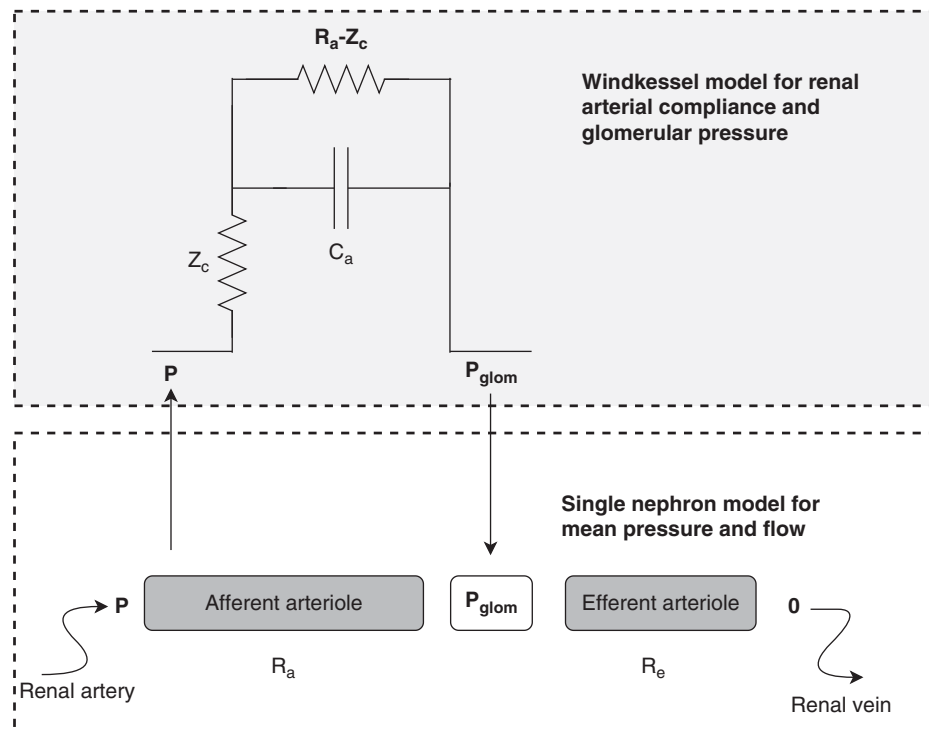


Figure 1. Schematic representation of the renal Windkessel model used to estimate glomerular pressure. The upper panel depicts the Windkessel model, which is fitted to match the relation between pressure and flow in the afferent arteriole. The lower panel depicts the Windkessel embedded in the single-nephron model for the estimation of the efferent resistance R_e . After the estimation of R_a and P_{glom} using the Windkessel model, R_e can be derived by $R_e = \frac{P_{glom} - 0}{F(0)}$. P is the pressure inside the main renal artery, Z_c is the characteristic impedance of the proximal renal artery, C_a is the renal artery compliance, R_a is the afferent resistance, and R_e is the efferent resistance.

afferent and efferent resistance and compliance. The fitted parameters derived from the model allowed estimation of P_{glom} , afferent and efferent resistances, and renal artery compliance in a heterogeneous population of patients with a clinical indication for renal or coronary angiography. In accordance with present knowledge, we found that patients with an increased perfusion pressure and patients with a history of diabetes had significantly higher estimates of P_{glom} .⁴ However, there was significant heterogeneity in estimated P_{glom} in both participants with and without diabetes, suggesting the possibility of identifying groups with and without adequate autoregulation on the basis of a lower or elevated P_{glom} . This is comparable with results showing an impaired renal autoregulation in different animal models of CKD.¹²

In this study, P_{glom} was on average 48 mm Hg. In animal models, glomerular pressure can be measured indirectly using stop-flow techniques or directly by micropuncture of nephrons; the work by Denton and Anderson³¹ has an overview of the available data.³² Micropuncture techniques provide a true, direct measurement of P_{glom} , but are limited to species with superficial nephrons, such as rats (48–56 mm Hg), squirrel monkeys (48.5 mm Hg), and rabbits (31–35 mm Hg).^{31,33,34} In these models, the glomerular pressure relative to systemic pressure was between 45% and 50%, similar to the value (46%) in this study. In humans, measurements of glomerular

filtration and filtration fraction are possible using tracers such as ¹²⁵I-iothalamate or inulin. However, this only allows assessment of whole-kidney hyperfiltration. To illustrate, a recent biopsy study of Denic *et al.*³⁵ in healthy kidney donors with normal renal function showed that glomerulosclerosis was associated with a higher single-nephron GFR but not with total GFR. Finally, it is possible to obtain an estimated P_{glom} using the Gomez equations as reviewed by Bjornstad *et al.*²³ These start from the assumption that normal glomerular pressure is 60 mm Hg and can therefore only provide a relative estimate.¹⁵ A major determinant in the Gomez equations is the gross filtration coefficient (*i.e.*, the number of milliliters per minute ultrafiltrate for each 1 mm Hg pressure), which is dependent on the structural aspects of the renal parenchyma. In applications of the Gomez equations, commonly a single fitted population average for this parameter without individual corrections for BP and kidney mass is used, which can affect the gross filtration coefficient. This makes the Gomez equations more suitable for determining changes after an intervention or to assess clinical correlates in a homogenous cohort.^{23,36} This can be improved by determining an individual gross filtration coefficient using sieving studies with a tracer such as dextran. In our analysis, we found no correlation between the Gomez equations and the Windkessel method, which can be attributed to the heterogeneity of our cohort, the use of an average

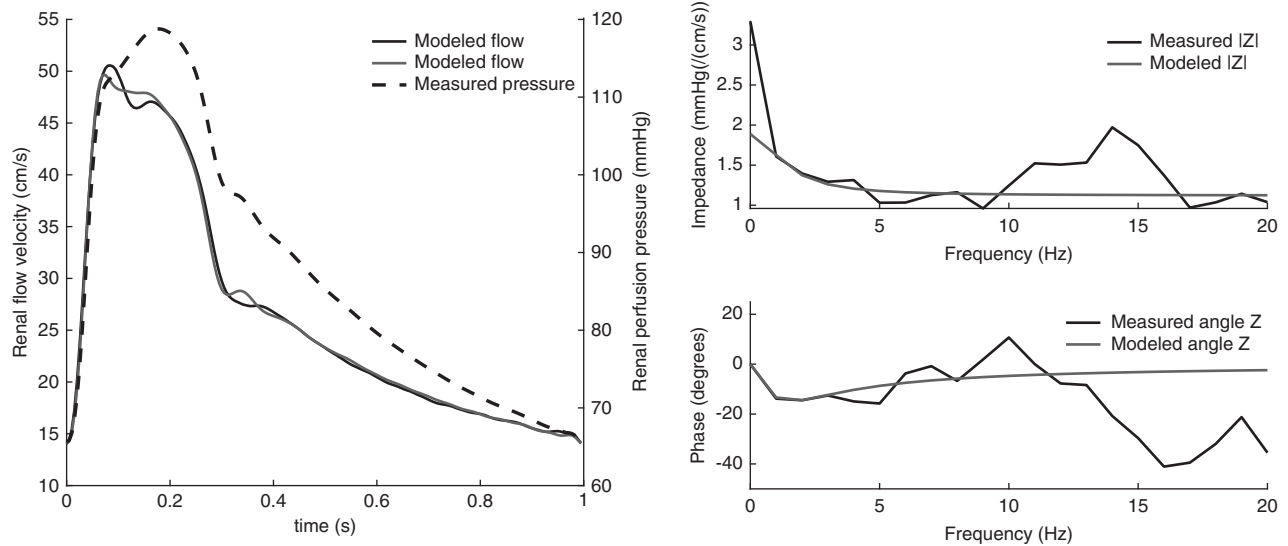


Figure 2. Representative example of a Windkessel fit during baseline. Black indicates the measured value, and gray indicates the fitted values. The left panel shows measured pressure, measured flow, and the modeled flow. The right panel shows measured and modeled impedance. In this example, the Windkessel fit resulted in a glomerular pressure of 37.4 mm Hg, a characteristic impedance of 1.12 mm Hg/(cm/s), and a compliance of 1.06 cm/mm Hg. The measured impedance and the fitted impedance differ in the direct current component due to the subtraction of the estimated Pglom in the modeled impedance. The shape of the absolute value and the phase of the modeled impedance and estimated impedance in this example are representative of an adequate measurement.

gross filtration coefficient, and the use of eGFR to estimate renal function. Our model gives a direct estimate of average glomerular pressure within a single kidney. This could be used in research to identify participants with hyperfiltration because an elevated glomerular pressure likely reflects increased single-nephron perfusion pressure and filtration.

We induced hyperemia using dopamine, which has a direct vasodilatory effect on both the afferent and efferent arterioles.^{37,38} Our results show that intrarenal administration of 30 $\mu\text{g}/\text{kg}$ dopamine induces an 88% increase in renal blood flow; this leads to a 43% decrease in afferent resistance and a more profound decrease of 62% in efferent resistance, causing Pglom to fall. Earlier studies in a dog model and the dose-response study by Manoharan *et al.*³⁹ have shown that this leads to maximal renal vasodilation, with few systemic effects.⁴⁰ This could explain the decrease in glomerular pressure after intrarenal dopamine. In contrast, systemic administration of dopamine leads to a lower increase in renal blood flow, with a large increase in systemic BP. In healthy volunteers, a systemic dose of 1.5–2.0 $\mu\text{g}/\text{kg}$ has been shown to yield increased renal blood flow and GFR but reduced filtration fraction. This suggests that dopamine has a relatively stronger dilatory effect on efferent arterioles in humans.^{41,42} We found a large dispersion in the hyperemic response to dopamine, both in incremental flow velocity and in arterial compliance and impedance, but Pglom decreased to a similar extent in all participants. Because the resulting Pglom was not dependent on perfusion pressure, this suggests that maximal vasodilation of the efferent arteriole was reached, resulting in lowering of Pglom close to the minimal required pressure for glomerular

ultrafiltration. Our own results showed that a second dosage of dopamine leads to the same reproducible maximal flow velocity even when the washout of the first dosage is not complete.¹⁸ In line, repeated intrarenal administration of dopamine resulted in a similar decrease in Pglom. Comparable with findings in animal models and human studies, we found that increases in Pglom were associated with an increase in perfusion pressure, presence of diabetes, and BMI. Animal models have shown that spontaneously hypertensive rats have a higher Pglom, whereas estimates in humans on the basis of the Gomez equations showed a comparable relation between mean arterial pressure and estimated Pglom pressure in patients with renovascular hypertension.^{14,36} The observed association between Pglom and diabetes corresponds with previous findings in a rat model of type 2 diabetes and a review of patient studies demonstrating an Pglom of 60 mm Hg in patients with type 2 diabetes relative to 52 mm Hg in controls using the Gomez equations.^{23,43} Similarly, the correlation between Pglom and BMI is comparable with other findings describing the relation with glomerular hyperfiltration and obesity.²

The limitation is that the obtained results are dependent on the validity of the model. The model is on the basis of the assumption that all glomeruli are functionally equal, resulting in one averaged Pglom. Animal models have shown that single-nephron glomerular filtration differs between cortical and medullary nephrons.⁴⁴ In addition, there could be regional differences between poles of the kidney. The derived variables are estimated for the whole kidney and thus, are likely not the same as the directly measured single-nephron values in animal models. Because we detected significant

Table 1. Baseline characteristics of the patients included in this analysis

Characteristics	Successful Fit	No Successful Fit
<i>n</i>	28	6
Age	59.0 [52.8–64.2]	53.5 [50.5–65.5]
Men, <i>n</i> (%)	21 (75.0)	2 (33.3)
BMI, mean (SD)	26.6 (4.1)	29.4 (4.9)
Office systolic BP, mm Hg, median [IQR]	138.5 [125.0–152.2]	155.5 [142.8–164.5]
Office diastolic BP, mm Hg, median [IQR]	74.0 [68.8–91.2]	82.5 [79.0–83.0]
History of diabetes, <i>n</i> (%)	10 (35.7)	1 (16.7)
History of cardiovascular disease, <i>n</i> (%)	19 (67.9)	4 (66.7)
History of smoking, <i>n</i> (%)	15 (53.6)	4 (66.7)
Plasma creatinine, mmol/L, median [IQR]	77.0 [67.8–94.5]	78.0 [68.8–85.8]
eGFR, ml/min per 1.73 m ² , median [IQR]	94.6 [74.4–98.6]	87.2 [63.9–100.0]
Plasma total cholesterol, mmol/L, mean (SD)	4.0 (0.9)	3.7 (0.7)
Plasma total LDL, mmol/L, mean (SD)	2.4 (0.7)	2.0 (0.5)
Microalbuminuria, <i>n</i> (%)	6 (26.1)	2 (50.0)
Use of ACE inhibitors or ARBs, <i>n</i> (%)	15 (53.6)	6 (100.0)
Use of antihypertensive medication, <i>n</i> (%)	20 (71.4)	6 (100.0)
RFR, median [IQR]	1.9 [1.6–2.6]	1.7 [1.6–1.9]
Renal artery stenosis, <i>n</i> (%)	3 (10.7)	1 (16.7)

RFR is defined as the hyperemic mean flow velocity divided by the baseline mean flow velocity. Data on albuminuria were available for 27 patients. ACE, angiotensin-converting enzyme; ARB, angiotensin receptor blocker; RFR, renal flow reserve.

associations with diabetes and BP in a relatively small and heterogeneous population, we consider the kidney-averaged values sensitive enough for making clinically relevant distinctions. We used the average of five to ten beats for the analysis to reduce measurement error in the pressure and flow signal and to account for changes in the flow signal resulting from respiratory-induced wire movements. Therefore, at present it is not possible to assess renal autoregulatory responses on a fast timescale using this technique. The model used only the data in the systole to enable estimation of P_{glom} in participants with a suboptimal flow signal during diastole; however, results were similar when applied to the complete heartbeat in participants with an optimal flow signal (data not shown). Additionally, although an advantage of the Windkessel method is that it was able to model the complex pulsatile pressure-flow relations in the renal artery, the inability to measure pressure or flow in or distal to the glomerulus required us to assume that pressure distal from the glomerulus was

constant. Multiple animal models have described the hydrostatic pressure profile along the different parts of the renal circulation from proximal to distal,⁴⁵ but there is a paucity of data on the morphology of the pulse wave. Studies in rat and dog models showed a similar but less pronounced pulsatile pattern in the glomerular capillary compared with the renal or femoral artery, whereas the pulsatility was completely absent distally from the glomerulus in the efferent arteriole.^{13,46} This would imply that the pulsatility of the arterial pressure is lost between the glomerulus and the efferent arteriole; therefore, the modeled P_{glom} could have underestimated true glomerular pressure. We believe that this difference is small and similar in all participants and that the modeled P_{glom} resembles the actual pressure. This should ideally be verified by direct comparison. The same assumption is used in

the hydrologic model by Rothe and Nash⁴⁷ to estimate renal arterial compliance in a dog model using an analog computer program. The efferent resistance in the model reflects the combined net resistance of the efferent arterioles and peritubular capillaries because measurement data to differentiate these components were not available. This does not affect the glomerular pressure or afferent resistance. The estimated P_{glom} in our model of the renal circulation is somewhat similar to the extrapolated critical closing pressure in the cerebral circulation, the differences being that the renal critical closing pressure is the pressure point necessary for glomerular ultrafiltration and that the cerebral closing pressure is the minimal pressure level for perfusion. However, in both cases, this is modeled as a pressure offset, which describes the minimal pressure to generate flow. To test model validity, we therefore also obtained an estimated P_{glom} by the first harmonic method used for estimating critical closing pressure in the cerebral circulation using mean pressure, mean flow, and the resistance

Table 2. Results of hemodynamic measurements and fitted Windkessel parameters: baseline versus hyperemia

Parameter	Baseline, Mean	SD	Hyperemia, Mean	SD	Difference ^a / Ratio ^b	L95	U95	P Value
Mean renal perfusion pressure, mm Hg	104.0	14.3	95.7	14.9	-8.3 ^a	-11.6	-5.0	<0.001
Flow velocity, cm/s	33.8	12.4	64.3	25.5	1.88 ^b	1.68	2.11	<0.001
Glomerular pressure, mm Hg	48.0	10.1	34.9	8.7	-13.1 ^a	-16.3	-10.0	<0.001
Afferent resistance, mm Hg/(cm/s)	1.86	0.75	1.07	0.50	0.57 ^b	0.49	0.65	<0.001
Efferent resistance, mm Hg/(cm/s)	1.63	0.72	0.65	0.33	0.38 ^b	0.32	0.44	<0.001
Characteristic impedance, mm Hg/(cm/s)	0.76	0.47	0.54	0.21	0.80 ^b	0.64	1.01	0.07
Compliance, cm/mm Hg	0.089	0.075	0.215	0.117	2.66 ^b	1.79	3.94	<0.001

L95, lower number of the 95% confidence interval; U95, upper number of the 95% confidence interval.

^aDenotes difference.

^bDenotes ratio, for which geometric mean and SD are given.

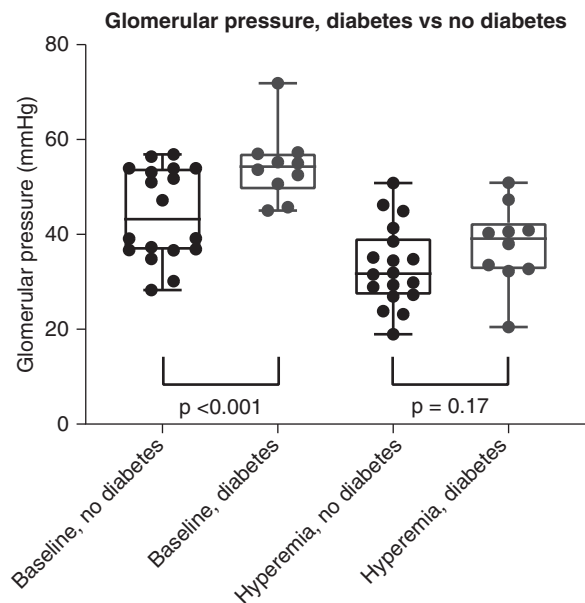


Figure 3. Distribution of estimated glomerular pressure under baseline (left) and hyperemic conditions (right) in patients with and without diabetes, showing a higher baseline P_{glom} in participants with diabetes. The boxes indicate medians and IQRs, and the bars indicate the ranges. *P* values show comparison of diabetes with nondiabetes mellitus corrected for renal perfusion pressure and BMI in a multiple linear regression model.

determined from the first harmonics. This showed a good agreement apart from a systematic bias.²⁸ However, the Windkessel method utilizes all harmonics of the signal, which additionally allows estimation of compliance and impedance. These have been used widely in the systemic and pulmonary circulation as measures of arterial stiffness and could thus be applied to the renal circulation to determine the effect of pulsatile flow.^{20,48}

In conclusion, we constructed a three-element renal Windkessel model that enables estimation of renal microvascular properties from invasively obtained intrarenal pressure and flow measurements. The comparable values of estimated P_{glom} with results obtained in animal models, the observed effects of dopamine on renal afferent and efferent resistance, and the obtained associations of intraglomerular with known clinical parameters support the usefulness of our model. In further research, it could be applied to assess the specific effects of different physiologic interventions and pharmacologic agents on renal hemodynamics in humans and may help us to better understand the renal hemodynamic consequences of CKD in patients receiving a percutaneous cardiac or renal intervention.

ACKNOWLEDGMENTS

Dr. Robbert de Winter, Dr. Jim A. Reekers, Dr. Peter M. van Brussel, Dr. Bert-Jan van den Born, and Dr. Liffert Vogt designed the original

study; Mr. Didier Collard, Dr. Robbert de Winter, Dr. Jan J. Piek, Dr. Jim A. Reekers, Dr. Peter M. van Brussel, Dr. Lennart van de Velde, and Dr. Gilbert W.M. Wijntjens performed the study measurements; Mr. Didier Collard, Dr. John M. Karemaker, Dr. Lennart van de Velde, and Dr. Berend E. Westerhof developed the adapted renal Windkessel model; Mr. Didier Collard performed data and statistical analyses; Mr. Didier Collard, Dr. Peter M. van Brussel, Dr. Lennart van de Velde, and Dr. Bert-Jan van den Born drafted and revised the paper; and Mr. Didier Collard, Dr. Robbert de Winter, Dr. John M. Karemaker, Dr. Jan J. Piek, Dr. Jim A. Reekers, Dr. Peter M. van Brussel, Dr. Lennart van de Velde, Dr. Bert-Jan van den Born, Dr. Liffert Vogt, Dr. Berend E. Westerhof, and Dr. Gilbert W.M. Wijntjens approved the final version of the manuscript. Dr. Jan J. Piek reports personal fees and non-financial support from Philips/Volcano, outside the submitted work.

DISCLOSURES

All authors have nothing to disclose.

FUNDING

This study was funded, in part, by an innovation grant (project number 19O118) from the Dutch Kidney foundation and by the involved medical departments.

SUPPLEMENTAL MATERIAL

This article contains the following supplemental material online at <http://jasn.asnjournals.org/lookup/suppl/doi:10.1681/ASN.2019121272/-/DCSupplemental>.

Supplemental Material.

Supplemental Figure 1. Bland–Altman analysis of the Windkessel method compared with the first harmonic method of estimation of glomerular pressure

Supplemental Figure 2. Comparison of estimated intraglomerular pressure using the Windkessel and Gomez method.

Supplemental Table 1. Results for univariate and multiple regression analyses for correlation of clinical characteristics with baseline estimated glomerular pressure.

REFERENCES

1. GBD 2015 DALYs and HALE Collaborators: Global, regional, and national disability-adjusted life-years (DALYs) for 315 diseases and injuries and healthy life expectancy (HALE), 1990–2015: A systematic analysis for the Global Burden of Disease Study 2015 [published correction appears in *Lancet* 389: e1, 2017]. *Lancet* 388: 1603–1658, 2016
2. Helal I, Fick-Brosnahan GM, Reed-Gitomer B, Schrier RW: Glomerular hyperfiltration: Definitions, mechanisms and clinical implications. *Nat Rev Nephrol* 8: 293–300, 2012
3. Rosenberg AZ, Kopp JB: Focal segmental glomerulosclerosis. *Clin J Am Soc Nephrol* 12: 502–517, 2017

4. Palatini P: Glomerular hyperfiltration: A marker of early renal damage in pre-diabetes and pre-hypertension. *Nephrol Dial Transplant* 27: 1708–1714, 2012
5. Fogo AB: Glomerular hypertension, abnormal glomerular growth, and progression of renal diseases. *Kidney Int Suppl* 75: S15–S21, 2000
6. Perkovic V, Agarwal R, Fioretto P, Hemmelgarn BR, Levin A, Thomas MC, et al.: Conference Participants: Management of patients with diabetes and CKD: Conclusions from a “Kidney Disease: Improving Global Outcomes” (KDIGO) Controversies Conference. *Kidney Int* 90: 1175–1183, 2016
7. Williams B, Mancia G, Spiering W, Agabiti Rosei E, Azizi M, Burnier M, et al.: ESC Scientific Document Group: 2018 ESC/ESH guidelines for the management of arterial hypertension. *Eur Heart J* 39: 3021–3104, 2018
8. Neuen BL, Young T, Heerspink HJL, Neal B, Perkovic V, Billot L, et al.: SGLT2 inhibitors for the prevention of kidney failure in patients with type 2 diabetes: A systematic review and meta-analysis. *Lancet Diabetes Endocrinol* 7: 845–854, 2019
9. van Bommel EJM, Muskiet MHA, van Baar MJB, Tonneijck L, Smits MM, Emanuel AL, et al.: The renal hemodynamic effects of the SGLT2 inhibitor dapagliflozin are caused by post-glomerular vasodilatation rather than pre-glomerular vasoconstriction in metformin-treated patients with type 2 diabetes in the randomized, double-blind RED trial. *Kidney Int* 97: 202–212, 2020
10. Cherney DZI, Perkins BA, Soleymanlou N, Maione M, Lai V, Lee A, et al.: Renal hemodynamic effect of sodium-glucose cotransporter 2 inhibition in patients with type 1 diabetes mellitus. *Circulation* 129: 587–597, 2014
11. Brenner BM: Hemodynamically mediated glomerular injury and the progressive nature of kidney disease. *Kidney Int* 23: 647–655, 1983
12. Carlström M, Wilcox CS, Arendshorst WJ: Renal autoregulation in health and disease. *Physiol Rev* 95: 405–511, 2015
13. Marchand GR: Direct measurement of glomerular capillary pressure in dogs. *Proc Soc Exp Biol Med* 167: 428–433, 1981
14. Komatsu K, Frohlich ED, Ono H, Ono Y, Numabe A, Willis GW: Glomerular dynamics and morphology of aged spontaneously hypertensive rats. Effects of angiotensin-converting enzyme inhibition. *Hypertension* 25: 207–213, 1995
15. Gómez DM: Evaluation of renal resistances, with special reference to changes in essential hypertension. *J Clin Invest* 30: 1143–1155, 1951
16. van Brussel PM, van de Hoef TP, de Winter RJ, Vogt L, van den Born B-J: Hemodynamic measurements for the selection of patients with renal artery stenosis: A systematic review. *JACC Cardiovasc Interv* 10: 973–985, 2017
17. Textor SC, Misra S, Oderich GS: Percutaneous revascularization for ischemic nephropathy: The past, present, and future. *Kidney Int* 83: 28–40, 2013
18. van Brussel PM, van Lavieren MA, Wijntjens GW, Collard D, van Lienden KP, Reekers JA, et al.: Feasibility and reproducibility of renal flow reserve with combined pressure and flow velocity measurements in humans [published online ahead of print April 9, 2019]. *Euro-Intervention* doi:10.4244/EIJ-D-18-01101
19. Cupples WA, Braam B: Assessment of renal autoregulation. *Am J Physiol Renal Physiol* 292: F1105–F1123, 2007
20. Saouti N, Westerhof N, Postmus PE, Vonk-Noordegraaf A: The arterial load in pulmonary hypertension. *Eur Respir Rev* 19: 197–203, 2010
21. Westerhof N, Lankhaar JW, Westerhof BE: The arterial Windkessel. *Med Biol Eng Comput* 47: 131–141, 2009
22. Updegrave A, Wilson NM, Merkow J, Lan H, Marsden AL, Shadden SC: SimVascular: An open source pipeline for cardiovascular simulation. *Ann Biomed Eng* 45: 525–541, 2017
23. Bjornstad P, Škrtić M, Lytvyn Y, Maahs DM, Johnson RJ, Cherney DZI: The Gomez’ equations and renal hemodynamic function in kidney disease research. *Am J Physiol Renal Physiol* 311: F967–F975, 2016
24. Levey AS, Stevens LA, Schmid CH, Zhang YL, Castro AF 3rd, Feldman HI, et al.: CKD-EPI (Chronic Kidney Disease Epidemiology Collaboration): A new equation to estimate glomerular filtration rate. *Ann Intern Med* 150: 604–612, 2009
25. Novak V, Yang ACC, Lepicovsky L, Goldberger AL, Lipsitz LA, Peng CK: Multimodal pressure-flow method to assess dynamics of cerebral autoregulation in stroke and hypertension. *Biomed Eng Online* 3: 39, 2004
26. Savitzky A, Golay MJE: Smoothing and differentiation of data by simplified least squares procedures. *Anal Chem* 36: 1627–1639, 1964
27. Parker KH: An introduction to wave intensity analysis. *Med Biol Eng Comput* 47: 175–188, 2009
28. Panerai RB, Salinet ASM, Brodie FG, Robinson TG: The influence of calculation method on estimates of cerebral critical closing pressure. *Physiol Meas* 32: 467–482, 2011
29. Navar GL: Regulation of renal hemodynamics. *Adv Physiol Educ* 20: S221–S235, 1998
30. Westerhof N, Stergiopulos N, Noble MIM, Westerhof BE: *Snapshots of Hemodynamics: An Aid for Clinical Research and Graduate Education*, 3rd Ed., Berlin, Springer, 2010
31. Denton KM, Anderson WP: Glomerular ultrafiltration in rabbits with superficial glomeruli. *Pflugers Arch* 419: 235–242, 1991
32. Vallon V: Micropuncturing the nephron. *Pflugers Arch* 458: 189–201, 2009
33. Maddox DA, Deen WM, Brenner BM: Dynamics of glomerular ultrafiltration. VI. Studies in the primate. *Kidney Int* 5: 271–278, 1974
34. Brenner BM, Troy JL, Daugharty TM: The dynamics of glomerular ultrafiltration in the rat. *J Clin Invest* 50: 1776–1780, 1971
35. Denic A, Mathew J, Lerman LO, Lieske JC, Larson JJ, Alexander MP, et al.: Single-nephron glomerular filtration rate in healthy adults. *N Engl J Med* 376: 2349–2357, 2017
36. Kimura G, London GM, Safar ME, Kuramochi M, Omae T: Glomerular hypertension in renovascular hypertensive patients. *Kidney Int* 39: 966–972, 1991
37. ter Wee PM, Donker AJM: Pharmacologic manipulation of glomerular function. *Kidney Int* 45: 417–424, 1994
38. Edwards RM: Response of isolated renal arterioles to acetylcholine, dopamine, and bradykinin. *Am J Physiol* 248: F183–F189, 1985
39. Manoharan G, Pijls NHJ, Lameire N, Verhamme K, Heyndrickx GR, Barbato E, et al.: Assessment of renal flow and flow reserve in humans. *J Am Coll Cardiol* 47: 620–625, 2006
40. McNay JL, McDonald RH Jr., Goldberg LI: Direct renal vasodilatation produced by dopamine in the dog. *Circ Res* 16: 510–517, 1965
41. ter Wee PM, Tegzess AM, Donker AJM: Pair-tested renal reserve filtration capacity in kidney recipients and their donors. *J Am Soc Nephrol* 4: 1798–1808, 1994
42. van Londen M, Kasper N, Hessels NR, Messchendorp AL, Bakker SJL, Sanders JS, et al.: Renal functional reserve capacity before and after living kidney donation. *Am J Physiol Renal Physiol* 315: F1550–F1554, 2018
43. Hashimoto S, Yamada K, Kawata T, Mochizuki T, Schnermann J, Koike T: Abnormal autoregulation and tubuloglomerular feedback in pre-diabetic and diabetic OLETF rats. *Am J Physiol Renal Physiol* 296: F598–F604, 2009
44. Steinhausen M, Endlich K, Wiegman DL: Glomerular blood flow. *Kidney Int* 38: 769–784, 1990
45. Maddox DA, Deen WM, Brenner BM: Glomerular filtration. In: *Handbook of Physiology—Section 8: Renal Physiology*, edited by Windhager EE, New York, Oxford University Press, 1992, pp 545–639
46. Drumond MC, Deen WM: Analysis of pulsatile pressures and flows in glomerular filtration. *Am J Physiol* 261: F409–F419, 1991
47. Rothe CF, Nash FD: Renal arterial compliance and conductance measurement using on-line self-adaptive analog computation of model parameters. *Med Biol Eng* 6: 53–69, 1968
48. McVeigh GE, Bratteli CW, Morgan DJ, Alinder CM, Glasser SP, Finkelstein SM, et al.: Age-related abnormalities in arterial compliance identified by pressure pulse contour analysis: Aging and arterial compliance. *Hypertension* 33: 1392–1398, 1999

AFFILIATIONS

¹Department of Vascular Medicine, Amsterdam University Medical Centers, University of Amsterdam, Amsterdam, The Netherlands

²Department of Cardiology, Amsterdam University Medical Centers, University of Amsterdam, Amsterdam, The Netherlands

³Faculty of Science and Technology, Technical Medical Centre, Multi-Modality Medical Imaging Group, University of Twente, Enschede, The Netherlands

⁴Faculty of Science and Technology, Technical Medical Centre, Cardiovascular and Respiratory Physiology, University of Twente, Enschede, The Netherlands

⁵Department of Medical Biology, Section Systems Physiology, Amsterdam University Medical Centers, University of Amsterdam, Amsterdam, The Netherlands

⁶Department of Radiology, Amsterdam University Medical Centers, University of Amsterdam, Amsterdam, The Netherlands

⁷Department of Nephrology, Amsterdam University Medical Centers, University of Amsterdam, Amsterdam, The Netherlands

Estimation of intraglomerular pressure using invasive renal arterial pressure and flow velocity measurements in humans

D. Collard^a, P.M. van Brussel^b, L. van de Velde^{a,c}, G.W.M. Wijntjens^b, B.E. Westerhof^d, J.M. Karemaker^e, J.J. Piek^b, J.A. Reekers^f, L. Vogt^g, R.J. de Winter^b, B.J.H van den Born^a

Supplemental Material

Supplement 1: Results for univariate and multiple regression analysis for correlation of clinical characteristics with baseline estimated glomerular pressure. [page 2](#)

Supplement 2: Bland-Altman analysis of Windkessel method compared to first harmonic method of estimation of glomerular pressure. [page 3](#)

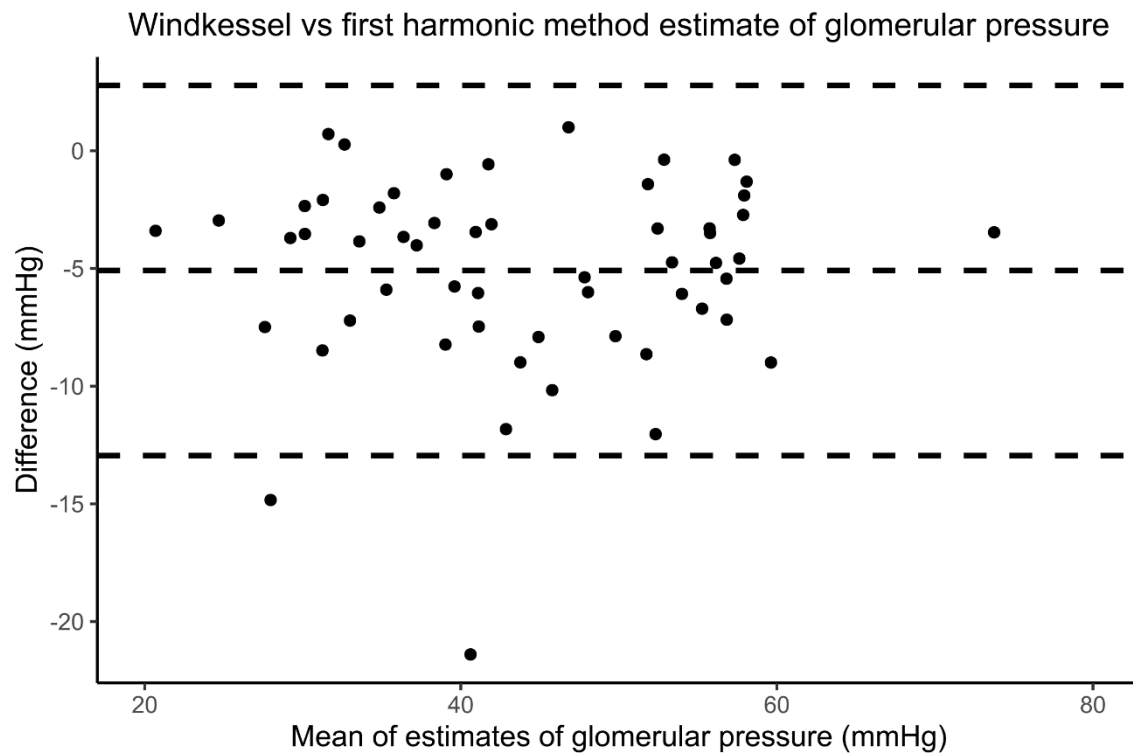
Supplement 3: Comparison of Windkessel model with Gomez equations [page 4](#)

Supplement 1: Results for univariate and multiple regression analysis for correlation of clinical characteristics with baseline estimated glomerular pressure.

Characteristic	Univariate linear regression					Multiple linear regression			
	Coef	L95	U95	P-value	R ²	Coef	L95	U95	P-value
Age	-0.04	-0.39	0.30	0.796	0.003				
Sex	3.21	-5.94	12.37	0.477	0.020				
BMI (kg/m ²)	0.77	-0.17	1.71	0.103	0.099	0.99	0.38	1.59	0.003
eGFR (ml/min/1.73m ²)	0.01	-0.21	0.24	0.894	0.001				
Microalbuminuria	4.69	-5.61	14.99	0.355	0.041				
History of diabetes	10.13	2.84	17.42	0.008	0.239	10.11	5.10	15.13	<0.001
Use of an ACE-inhibitor or ARB	4.22	-3.62	12.06	0.278	0.045				
Renal perfusion pressure (mmHG)	0.36	0.12	0.61	0.005	0.260	0.42	0.25	0.60	<0.001

Supplementary table 1: Results for univariate and multiple regression analysis for correlation of clinical characteristics with baseline estimated glomerular pressure. BMI denotes body mass index, eGFR estimated glomerular filtration rate, ACE angiotensin converting enzyme, ARB angiotensin receptor blocker. Coef denotes the regression coefficient, L95 and U95 indicate the 95% confidence interval.

Supplement 2: Bland-Altman analysis of Windkessel method compared to first harmonic method of estimation of glomerular pressure.



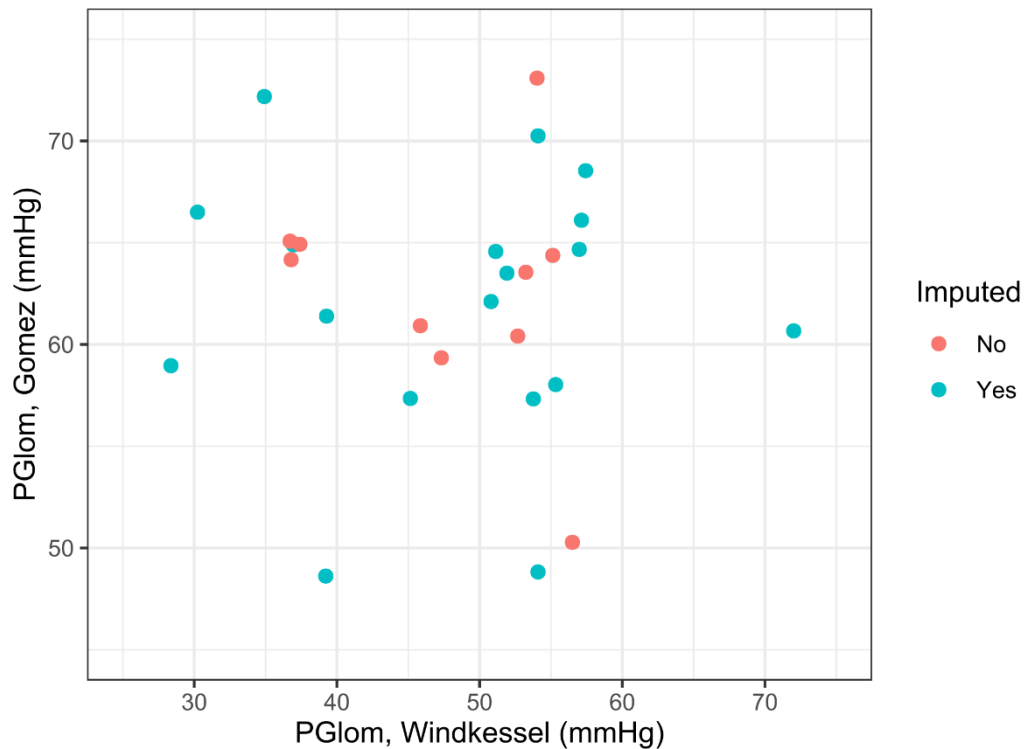
Supplemental figure S1: Bland-Altman analysis of Windkessel method compared to first harmonic method of estimation of glomerular pressure. The Windkessel method is on average 5.1 mmHg lower (95% CI of difference $-13.0 - 2.8$), with good overall agreement (ICC 0.94, $p < 0.001$).

Supplement 3: Comparison of Windkessel model with Gomez' equations

In a subset of 10 of the 28 participants, we pressure-flow measurements were performed in the main branch of the renal artery and we could estimate renal blood flow using intrarenal flow velocity and the diameter of the main artery. In the other participants either a measurement in a branch of the renal artery was performed, or there was no reliable angiographic image available. The area of the renal artery was determined using Quantitative Coronary Angiography software (Medis – Qangio XA 7.3.54.0). The area of the vessel was used to estimate renal blood flow from renal blood flow velocity (using $\frac{1}{2} * \text{area} * \text{blood flow velocity}$ which assumes a Poiseuille flow profile), which we multiplied by 2 to determine total renal blood flow.¹ We then determined filtration fraction based on estimated glomerular filtration rate (based on the CKD-EPI formula using peri-procedural plasma creatinine), plasma hematocrit and renal blood flow. We determined the gross filtration coefficient Kfg by dividing the mean eGFR by 25 (assumed filtration pressure across capillaries, corresponding to a mean Pglom of 60). The glomerular oncotic pressure was determined from the estimated filtration fraction and the total plasma protein. Estimated glomerular pressure was then calculated using the Gomez' equations.^{2,3}

$$P_{glom} = \Delta P_{filt} + P_{Bowman} + P_{hydro} = \frac{GFR}{K_{fg}} + 5 \cdot \left[\frac{TP}{FF} \cdot \ln \left(\frac{1}{1 - FF} \right) - 2 \right] + 10$$

Both the Windkessel method and the Gomez' equations give estimates for glomerular pressure in the physiological range (50-73 for the Gomez' equations, 37-55 for Windkessel), but they have poor correlation (R: -0.24, 95%CI -0.75-0.46). As the major determinants of Pglom in the Gomez' equations are GFR, plasma protein and Kfg, we imputed in the other participants the filtration fraction using the mean (16.3), which gave a similarly poor correlation (R:-0.08, 95%CI -0.44 – 0.30) Supplementary figure 2 shows the comparison between the Windkessel method and the Gomez' equations.



Supplemental figure S2: Comparison of estimated intraglomerular pressure (Pglom) using the Windkessel and Gomez method. Blue dots are participants where filtration fraction was imputed, red dots are participants where filtration fraction was determined from GFR and renal plasma flow.

References

1. Doucette JW, Corl PD, Payne HM, Flynn AE, Goto M, Nassi M, Segal J: Validation of a Doppler guide wire for intravascular measurement of coronary artery flow velocity. *Circulation* 85: 1899–1911, 1992
2. Bjornstad P, Škrtić M, Lytvyn Y, Maahs DM, Johnson RJ, Cherney DZI: The Gomez equations and renal hemodynamic function in kidney disease research. *Am. J. Physiol. Physiol.* 311: F967–F975, 2016
3. Tonneijck L, Smits MM, Muskiet MHA, Hoekstra T, Kramer MHH, Danser AHJ, Ter

Estimation of intraglomerular pressure in humans

Wee PM, Diamant M, Joles JA, Van Raalte DH: Renal effects of DPP-4 inhibitor sitagliptin or GLP-1 receptor agonist liraglutide in overweight patients with type 2 diabetes: A 12-week, randomized, double-blind, placebo-controlled trial. *Diabetes Care* 39: 2042–2050, 2016